A linearized branch flow model considering line shunts for radial distribution systems and its application in Volt/VAr control

Lin, Hanyang; Ul Nazir, Firdous; Pal, Bikash C.; Guo, Ye

Published in:
Journal of Modern Power Systems and Clean Energy

DOI:
10.35833/MPCE.2022.000382

Publication date:
2023

Document Version
Publisher's PDF, also known as Version of record

A Linearized Branch Flow Model Considering Line Shunts for Radial Distribution Systems and Its Application in Volt/VAr Control

Hanyang Lin, Firdous Ul Nazir, Bikash C. Pal, and Ye Guo

***Abstract*—When urban distribution systems are gradually modernized, the overhead lines are replaced by underground cables, whose shunt admittances can not be ignored. Traditional power flow (PF) model with π equivalent circuit shows non-convexity and long computing time, and most recently proposed linear PF models assume zero shunt elements. All of them are not suitable for fast calculation and optimization problems of modern distribution systems with non-negligible line shunts. Therefore, this paper proposes a linearized branch flow model considering line shunt (LBFS). The strength of LBFS lies in maintaining the linear structure and the convex nature after appropriately modeling the π equivalent circuit for network equipment like transformers. Simulation results show that the calculation accuracy in nodal voltage and branch current magnitudes is improved by considering shunt admittances. We show the application scope of LBFS by controlling the network voltages through a two-stage stochastic Volt/VAr control (VVC) problem with the uncertain active power output from renewable energy sources (RESs). Since LBFS results in a linear VVC program, the global solution is guaranteed. Case study exhibits that VVC framework can optimally dispatch the discrete control devices, viz. substation transformers and shunt capacitors, and also optimize the decision rules for real-time reactive power control of RES. Moreover, the computing efficiency is significantly improved compared with that of traditional VVC methods.**

***Index Terms*—Line shunt, linear power flow model, stochastic optimization, Volt/VAr control (VVC).**

NOMENCLATURE

A. Sets and Indexes

B	Set of all the buses
Cap, RES	Sets of buses with capacitors and renewable energy sources (RESs)
i, j	Indices of buses i and j
s	Index of the s^{th} scenario
Trf	Set of branches with transformers

B. Parameters

ΔP_{RES}	Forecasted error of active power produced by RES
γ_{ij}	Coefficient of constant series impedance and shunt admittance of branch between buses i and j
d_j	Apparent load power at bus j
Gs, Bs	Shunt conductance and susceptance
$k_{\min}, k_{\max}$	The minimum and maximum voltage ratios of transformer
N_s	Number of scenarios
$P_{d,j}, Q_{d,j}$	Active and reactive load power at bus j
P^s_{RES}	Active power produced by RES
P^0_{RES}	Forecasted value of active power produced by RES
$Q_{cap,\max}$	The maximum reactive power available from shunt capacitor bank
$Q_{RES,\min}$, $Q_{RES,\max}$	The minimum and maximum reactive power produced by RES
r_{ij}, x_{ij}	Series resistance and reactance of branch between buses i and j
$V_{\min}, V_{\max}$	The minimum and maximum nodal voltage magnitudes
y_i, y_j	Line shunt admittance magnitudes at buses i and j
y_{ij}	Shunt admittance magnitude of branch between buses i and j at bus i, $y_{ij} = 1/z_{ij}$
y_{i0}, y_{j0}	Equivalent shunt admittances of transformer at buses i and j
y^s_{ij}	Series admittance magnitude of transformer located at branch between buses i and j at bus i
y^m_{ij}	Shunt excitation admittance magnitude of transformer located at branch between buses i and j at bus i
z_{ij}	Series impedance magnitude of branch between buses i and j

Manuscript received: June 30, 2022; revised: October 15, 2022; accepted: February 5, 2023. Date of CrossCheck: February 5, 2023. Date of online publication: February 24, 2023.

The work of H. Lin and Y. Guo was supported in part by the National Natural Science Foundation of China (No. 51977115).

H. Lin and Y. Guo are with Tsinghua-Berkeley Shenzhen Institute, Shenzhen International Graduate School, Tsinghua University, Shenzhen 518071, China (e-mail: Linhy22@mails.tsinghua.edu.cn; guo-ye@sz.tsinghua.edu.cn).

F. U. Nazir (corresponding author) is with the Department of Electrical and Electronic Engineering, Glasgow Caledonian University, Glasgow, G4 0BA, U.K. (e-mail: firdousul.nazir@gcu.ac.uk).

B. C. Pal is with the Department of Electrical and Electronic Engineering, Imperial College London, London, SW7 2AZ, U.K. (e-mail: b.pal@imperial.ac.uk).

DOI: 10.35833/MPCE.2022.000382

C. Variables

ΔQ_{RES}	Reactive power adjustment by RES in response to its active power fluctuation
ΔV_{ij}	Voltage magnitude drop between buses i and j
d_j^s	Apparent load power at bus j for each scenario
f_{ij},f_{jk}	Branch current magnitudes flowing through series impedance between buses i and j and other connecting buses
f_i^+,f_i^-	Sending- and receiving-end branch current magnitudes at bus i
f_j^+,f_j^-	Sending- and receiving-end branch current magnitudes at bus j
f_j^{+s},f_j^{-s}	Sending- and receiving-end branch current magnitudes at bus j for each scenario
k	Transformer voltage ratio
$loss_{adj}$	Expected power loss of adjustable case
$loss_{det}$	Expected power loss of deterministic case
n_{VVs}	Number of voltage violations
N_B	Number of nodes
N_{sVV}	Number of scenarios with at least one voltage violation
Q_{cap}	Reactive power from shunt capacitor bank
$Q_{cap,j}$	Reactive power from shunt capacitor bank at bus j
$Q_{RES,j}$	Reactive power produced by RES
$Q_{RES,j}^0$	Reactive power produced by RES in deterministic case at bus j
t_j	Epigraph transformation factor at bus j
V_i, V_j	Voltage magnitudes at buses i and j

D. Function

$Obj(\cdot)$	Objective function

I. Introduction

POWER flow is the most important component of many power system problems such as planning and optimization problems for transmission and distribution systems. As modern power systems are evolving into highly complex entities owing to huge integration of renewable energy sectors and fast expansion of network applications, the selection of a proper power flow (PF) model is of key concern.

The most commonly used PF model is called alternating current PF (ACPF), which is non-linear. The traditional optimization problems based on ACPF would be non-convex, hard to solve, and time-consuming [1]. Therefore, various simplified models [2] - [9] have been proposed to overcome these problems with different characteristics of distribution systems. Though many simplified models have achieved excellent results, some of them are non-linear or require iterative algorithms for their solution [10]. This not only results in difficulties for solving optimization problems but also lacks efficiency in terms of computing times [11].

In order to achieve higher efficiency to solve PF and relevant optimization problems quickly, this paper chooses a previously analyzed linearized branch flow (LBF) model with fast computating speed and acceptable accuracy [12]. LBF model is adapted from a linearized network model of direct current load flow in [13], and is also mentioned as a similar version called a direct approach for PF solutions in [14]. However, both these versions of LBF model in [13] and [14] do not consider line shunts.

As for real radial distribution systems, various network equipments like transformers, capacitors, and distributed generation, mainly renewable energy source (RES), are present, and each branch not only has series impedance but also has shunt admittance. Several branch flow models proposed in [15] - [17] ignore these shunt elements, which means that there is no π-structure circuit line model in these branch flow models. These models can be accepted in previous years when the majority of distribution lines are overhead lines with relatively small shunt admittance. However, according to [18] and a field test report from Shenzhen Power Supply Company, China, when distribution systems are gradually modernized, the overhead lines are replaced by underground cables, whose shunt admittance is 5-10 times larger [19], [20]. Therefore, shunt elements cannot be negligible anymore in modern PF analysis.

There are three main previous studies [21] - [23] that have proposed different formulations of DistFlow model and branch flow model with non-zero line shunts. A branch flow model is proposed in [21] that includes non-zero line shunts, and a local algorithm is also provided to compute a local optimal of optimal PF (OPF) problems. Another branch flow model with non-zero line shunts is proposed in [22], which is a more conservative approximation of ACPF. A sufficient condition for the SOCP relaxation of the approximate OPF to be exact is also provided in [22]. Reference [23] proposes an alternative branch flow model with non-zero line shunts, and proves that the equivalence and the exactness of second-order cone relaxation continue to hold under essentially the same conditions as when line shunts are zero. All of the aforementioned models are not linear, thus loosing the computing efficiency in the calculation of large distribution systems.

This paper proposes an alternative LBF model with non-zero line shunts (LBFS), which is the π equivalent circuit model for LBF. LBFS continues to hold the strength of short computing time under the same computing conditions as zero line shunts. Furthermore, LBFS is expanded to include transformers.

The "charging effect" caused by non-negligible capacitive susceptance of shunt admittance would lift the nodal voltage magnitude at certain nodes, potentially cause the risk of voltage violations, and affect the safe operation and reliability in modern distribution systems. Therefore, our essential purpose of applying Volt/VAr control (VVC) is to maintain nodal voltage in the acceptable range, avoid the violations of load power constraints, and provide additional reactive power from capacitors and RESs to the bulk distribution system [24]. Usually, shunt capacitors [25], transformers, and distributed generators are employed for VVC to achieve these aims [26].

Most VVC strategies implement a centralized controller

which decides the optimum set points of controllable devices based on current network topology and net nodal injections [24]. Some methods are proposed to solve the centralized VVC problem, like interior point method [27], mixed-integer linear programming [28], dynamic programming [29] and evolutionary algorithm [30]. Some studies have proposed different optimal control methods of reactive power to improve the voltage regulation. A Volt/VAr optimization method which operates in complex variables based on the Wirtinger calculus is proposed in [31]. A two-stage chance-constrained optimization problem is solved in [24] to handle nodal power uncertainties. However, the VVC problem based on ACPF is computationally expensive and may require several hours to solve in a large-scale network, thereby making it practically not useful. Also, VVC problems based on linear PF models without the modeling of line shunts are not applicable for modern distribution systems with underground cables.

As LBFS results in a linear mathematical structure, the storage memory space and solving time are hugely saved. Since LBFS shows the superiority in accuracy of voltage magnitude and computing efficiency with the modeling of non-zero line shunts and transformers, we construct a linear two-stage stochastic optimization formulation for VVC problem which is significantly faster than traditional methods and makes operating points free of voltage violations.

The schedules of the discrete controlling devices are held at fixed settings throughout the entire optimization horizon (an hour time window), while the inverter reactive powers are adjusted in the second stage, upon the final revelation of uncertainty according to the decision rule connecting active and reactive powers of RES.

The major contributions of the paper are two-fold:

1) LBFS is proposed as the first linear PF model with π equivalent circuit to consider non-zero line shunts and shunt excitation admittance of the transformer. The distribution lines and transformers naturally admit a π equivalent circuit model, but they are non-convex and cannot be applied directly. The strength of LBFS lies in its linear and simple mathematical structure. After introducing a system fixed factor γ in the voltage drop equation, the proposed LBFS model achieves an enhanced accuracy in nodal voltage magnitude and branch current magnitude compared with the widely used linear DistFlow and LBF model under the benchmark solved by ACPF, while maintaining the fast computating efficiency which is typical of LBF.

2) A two-stage VVC problem is proposed to control the nodal voltage magnitude and avoid the voltage violations caused by "charging effect" from shunt elements and nodal power injection from distributed RES units. A linear decision rule is introduced to adjust the real-time reactive power according to the active power forecasted errors. The whole optimization scheme based on LBFS results in a linear structure and therefore is easily implemented. The proposed VVC problem has a better performance in eliminating voltage violations than the traditional deterministic case and exhibits a fast computing efficiency compared with traditional VVC problems based on ACPF.

The rest of the paper is organized as follows. Section II introduces the model formulation. Section III constructs a two-stage linear stochastic VVC problem based on LBFS and describes the linearity and convexity of the framework. Section IV provides the numerical results on three test systems. The paper is concluded in Section V.

II. Model Formulation

A. LBF Model with Line Shunts

LBF model is adapted from linearized network model of direct current load flow [13], [14], and is visualized in a part of a radial distribution system as shown in Fig. 1. $f_{ij}=f_j^-$ because LBF assumes no power loss on the series impedance.

$$f_j^- = d_j + f_j^+ \tag{1}$$

$$V_i = V_j + z_{ij} f_{ij} \tag{2}$$

$$d_j = \left| P_{d,j} + \mathrm{j} Q_{d,j} \right| \tag{3}$$

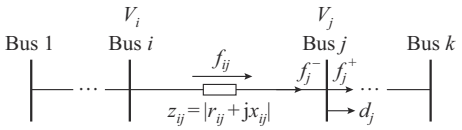

Fig. 1. Part of a radial distribution system.

In (1), the magnitude of complex load power is set as the branch current magnitude, so the current injections satisfy Kirchoff's current law (KCL). In (2), $\Delta V_{ij}=V_i-V_j$ is the product of the magnitude of line impedance and branch current, satisfying Ohm's law. Besides, the accuracy and application scope analyses of LBF model for radial distribution systems are proposed by [12].

Next, consider the branch flow model of a radial distribution system with π equivalent circuit model shown in Fig. 2. The majority of the model is the same as LBF with the same meaning and symbol of parameters. However, the main difference is the distribution line from bus i to bus j is represented by a π equivalent circuit model. The π equivalent circuit model includes three elements z_{ij}, y_i, y_j. Since this LBF model with line shunts does not consider transformers, we make a practical assumption that $y_i=y_j=y_{ij}/2$.

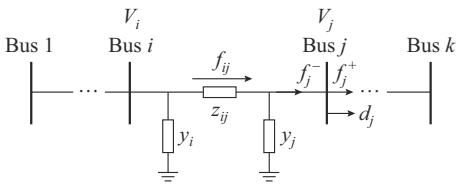

Fig. 2. Part of a radial distribution system with π equivalent circuit model.

According to the LBFS model shown in Fig 2, the current flowing through z_{ij} from bus i to bus j can be expressed as:

$$f_{ij} = f_j^- + V_j y_{ij}/2 \tag{4}$$

Then, the voltage magnitude at bus i can be obtained as:

$$V_i = V_j + z_{ij} f_{ij} = V_j + z_{ij}\left(f_j^- + V_j y_{ij}/2 \right) = V_j + z_{ij} f_j^- + V_j z_{ij} y_{ij}/2 = \left(1 + z_{ij} y_{ij}/2\right) V_j + z_{ij} f_j^- \tag{5}$$

Therefore, the formulation of LBFS model is given as:

$$f_j^- = d_j + f_j^+ \tag{6}$$

$$V_i = \gamma_{ij} V_j + f_j^- z_{ij} \tag{7}$$

$$\gamma_{ij} = 1 + z_{ij} y_{ij}/2 \tag{8}$$

Obviously, (6) obeys the KCL, while (7) represents the Ohm's law. The LBFS model preserves the mathematical structure as LBF model by setting the coefficient of V_j equal to a parameter denoted by γ_{ij}, known as the system fixed factor. It is important to note that the fixed parameter of the system depends on the line impedance and shunt admittance magnitudes, and hence remains fixed for different operating conditions. LBFS still holds its simplicity without involving iterative and complex parts.

B. Transformer Modeling

This paper models the shunt capacitors with Q_{Cap}. Also, we assume the value remains constant for a particular operating state, which is reasonable and makes the model formulation simple. The reactive power compensation from capacitors can supply leading var and maintain the voltage in the stable region.

The traditional distribution systems usually have transformers located in the substation nodes to change feeder voltage levels [32]. However, transformers or voltage regulators may also be located in other branches in some special scenarios. Thus, we consider both conditions and formulate the transformer model considering transformer voltage ratio k within a branch where a transformer is located.

The original equivalent circuit of an ideal transformer located between buses i and j is visualized in Fig. 3. z_{ij} and y_{ij}^m are considered at the lower voltage side. The line impedance and admittance are ignored in the transformer modeling because the bus j is the fictitious bus for transformers. Obviously, the power flowing in and out the ideal transformer should be the same.

$$V_i f_i^+ = \frac{1}{k} V_i \left(f_j^- + V_j y_{ij}^m \right) \tag{9}$$

$$f_i^+ = \frac{1}{k} \left(f_j^- + V_j y_{ij}^m \right) \tag{10}$$

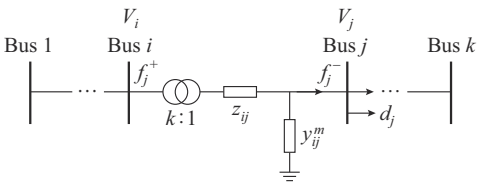

Fig. 3. Original equivalent circuit of ideal transformer in part of a radial distribution system.

Also, the voltage change at both sides is given as:

$$V_i/k = V_j + \left(f_j^- + V_j y_{ij}^m \right) z_{ij} \tag{11}$$

The following equations are obtained by combining (10) and (11):

$$\begin{cases} f_i^+ = \dfrac{1}{z_{ij} k^2} V_i - \dfrac{1}{z_{ij} k} V_j \\ f_j^- = \dfrac{1}{z_{ij} k} V_i - \left(\dfrac{1}{z_{ij}} + y_{ij}^m \right) V_j \end{cases} \tag{12}$$

A π equivalent circuit is assumed to exist between buses i and j, which is defined by the following pair of equations:

$$\begin{cases} f_i^+ = \left(y_{i0} + y_{ij} \right) V_i - y_{ij} V_j \\ f_j^- = y_{ji} V_i - \left(y_{j0} + y_{ji} \right) V_j \end{cases} \tag{13}$$

By combining (12) and (13), we can obtain:

$$\begin{cases} y_{ij} = \dfrac{1}{z_{ij} k} \\ z_{ij} = z_{ij} k \\ y_{i0} = \dfrac{1-k}{k^2} y_{ij}^s \\ y_{j0} = \dfrac{k-1}{k} y_{ij}^s + y_{ij}^m \end{cases} \tag{14}$$

where $y_{ij} = y_{ji}$ shows the reciprocity of passive circuit of transformers; and $y_{ij}^s = 1/z_{ij}$. Thus, the transformer is modeled within the LBFS by considering the effect of the nominal tap ratios on the π equivalent circuit model, as shown in Fig. 4.

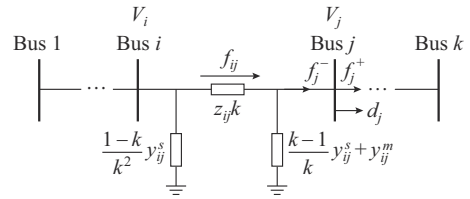

Fig. 4. π equivalent circuit of ideal transformer in part of a radial distribution system.

According to the LBFS model with transformers shown in Fig. 4, the current flowing through the series impedance $z_{ij}k$ in line from bus i to bus j can be expressed as:

$$f_{ij} = f_j^- + \left(\frac{k-1}{k} y_{ij}^s + y_{ij}^m \right) V_j \tag{15}$$

Then, we can obtain the voltage magnitude at bus i:

$$\begin{aligned} V_i &= V_j + f_{ij} z_{ij} k = V_j + \left(f_j^- + \left(\frac{k-1}{k} y_{ij}^s + y_{ij}^m \right) V_j \right) z_{ij} k = \\ &\left(1 + (k-1) z_{ij} y_{ij}^s + y_{ij}^m z_{ij} k \right) V_j + f_j^- z_{ij} k = \left(1 + y_{ij}^m z_{ij} \right) k V_j + f_j^- z_{ij} k \end{aligned} \tag{16}$$

Like the LBFS model, we set the coefficient of V_j equal to γ'_{ij}, known as the system fixed factor. Therefore, the LBF model with line shunts and transformers is given as:

$$f_j^- = d_j + f_j^+ \tag{17}$$

$$V_i = \gamma'_{ij} V_j + f_j^- z_{ij} k \tag{18}$$

$$\gamma'_{ij} = \left(1 + z_{ij} y_{ij}^m \right) k \tag{19}$$

Obviously, (17) obeys the KCL, while (18) represents the Ohm's law. LBFS with transformers still holds its simplicity

without involving non-linear parts.

III. Two-stage Linear Stochastic VVC Problem

A. Objective Function

As a traditional optimization problem, VVC is a minimization problem, whose constraints are mostly inequality type. Our goal is to find the global solution quickly without violating the constraints and limits:

$$Obj(1) = \left| V_j - 1 \right| \tag{20}$$

$$Obj(2) = t_j \quad -t_j \le V_j - 1 \le t_j \tag{21}$$

$Obj(1)$ represents the minimization of the difference between 1 p.u. and nodal voltage magnitude, in other words, the minimization of voltage deviation around the nominal voltage profile. We use the epigraph transformation with t_j of the objective function, as shown in $Obj(2)$, to avoid the absolute value sign for obtaining the linearity.

B. Problem Description

We set up a two-stage linear stochastic VVC problem based on the linear VVC framework. In the first stage, the slow controls, shunt capacitor banks, and the set points of transformer voltage ratio are "here and now" decisions, which should be made before the uncertainty of RES active power output is revealed, and kept fixed throughout the entire optimization interval (an hourly time window). As for the second stage, the fast controls viz. the reactive power from RES inverters are allowed to be "wait and see" decisions. The second stage adjusts the reactive power from the RES in real time according to a pre-defined rule. This predefined rule is chosen to be a linear equation relating the RES reactive power to its active power, whose coefficients are also available from the first stage. Previously, another linear rule adjusting the RES reactive power has been used in [33]. The linear rule to adjust the RES reactive power based on the active power prediction has the following form:

$$P^s_{RES,j} = P^0_{RES,j} + \Delta P^s_{RES,j} \tag{22}$$

$$Q^s_{RES,j} = Q^0_{RES,j} + \Delta Q^s_{RES,j} = Q^0_{RES,j} + m_j \Delta P^s_{RES,j} \tag{23}$$

The following assumptions are enforced while carrying out the optimization.

1) As for the discrete variables, i.e., reactive power from shunt capacitor banks $Q_{Cap,j}$ and transformer voltage ratio k_j, they would make the optimization problem a mixed-integer linear programming framework. To avoid this, we regard them as the continuous variable in the linear programming and subsequently round the final values to the nearest discrete values.

2) The load power equation considering the active power from RES units has the following expression:

$$d^s_j = \sqrt{\left[\left(P_{d,j} - \underbrace{P^0_{RES,j} - \Delta P^s_{RES,j}}_{P^s_{RES,j}} \right)^2 + Q_{d,j} \right]^2} \quad \forall j \in B \tag{24}$$

Equation (24) is constant because both the forecasted value and error of RES's active power are parameters. The reactive power from shunt capacitors and RES is placed in the current injection equation instead of the load equation to make the optimization problem tractable, because it would break the convexity and linearity by putting variables inside the square-root sign.

Also, we set fictitious buses in the branches where transformers are located to form the ideal transformer between the sending-end bus and fictitious bus. Thus, the two-stage linear stochastic VVC problem is shown as follows.

$$\min_{\mathcal{O}} t^s_j \tag{25}$$

s.t.

$$-t^s_j \le V^s_j - 1 \le t^s_j \quad \forall j \in B \tag{26}$$

$$V_{\min} \le V^s_j \le V_{\max} \quad \forall j \in B \tag{27}$$

$$0 \le Q_{Cap,j} \le Q_{Cap,\max} \quad \forall j \in Cap \tag{28}$$

$$Q_{RES,\min} \le \underbrace{Q^0_{RES,j} + m_j \Delta P^s_{RES,j}}_{Q^s_{RES,j}} \le Q_{RES,\max} \quad \forall j \in RES \tag{29}$$

$$f^{-s}_j = d^s_j - Q_{Cap,j} - \underbrace{\left(Q^0_{RES,j} + m_j \Delta P^s_{RES,j} \right)}_{Q^s_{RES,j}} + f^{+s}_j \quad \forall j \in B \tag{30}$$

$$V^s_j = \gamma'_j V^s_{j'} + f^{-s}_j z_{jj'} k \quad \forall j \in Trf \tag{31}$$

$$\gamma'_j = \left(1 + z_{jj'} y^m_{jj'} \right) k_j \quad \forall j \in Trf \tag{32}$$

$$k_{\min} \le k_j \le k_{\max} \quad \forall j \in Trf \tag{33}$$

$$V^s_i = \gamma_{ij} V^s_j + f^{-s}_j z_{ij} \quad \forall i,j \in B \tag{34}$$

$$\gamma_{ij} = 1 + z_{ij} y_{ij}/2 \quad \forall i,j \in B \tag{35}$$

The objective function is the minimization of voltage magnitude violation. The feasible region is demarcated by the constraints (26)-(35) and is defined by the vector of optimization variables $\mathcal{O} = \left[t^s_j, V^s_j, Q_{Cap,j}, Q^0_{RES,j}, f^s_{jk}, f^{s-}_j, k_j, m_j \right]^{\mathrm{T}}$. Formula (26) defines t^s_j for each scenario. Formula (27) describes the permitted operating range of nodal voltage magnitude for each scenario. Formulas (28) and (29) make sure that the reactive power from shunt capacitors and RES is respectively within their own limits for each scenario. The current injection for each scenario is defined by (30). Equation (31) denotes the voltage change at the branches where transformers are located, and bus j' is the fictitious bus. Equations (32) and (35) represent the system fixed factor at the fictitious node and rest nodes, respectively. The transformer voltage ratio should be within its limits as given by (33). Equation (34) describes the voltage drop at each bus for each scenario.

C. Solution Strategy

The two-stage linear stochastic VCC problem is proposed to decrease the probability of voltage violation with the uncertain nodal net injections from RES under the condition of "charging effect" from shunt elements. The large-size VVC problem, caused by the consideration of all generated scenarios, can be solved because of the proposed model. The first stage (deterministic case when $s = 1$) ignores the forecasted errors of RES as $\Delta P^s_{RES,j} = 0$ and gets the slow control settings of $Q_{cap,j}$, k_j, and $Q^0_{RES,j}$. As for the second stage, N_s

Gaussian scenarios along with $\Delta P^{s}_{RES,j}$ are generated randomly and used to solve the optimization problem, while the optimal solutions from the first stage, $Q_{cap,j}$, k_j, and $Q^{0}_{RES,j}$, are kept fixed. The real-time $Q^{s}_{RES,j}$ from RES inverters is optimally adjusted based on m_j and the forecasted errors of RES. Notice that m_j only contains a single value corresponding to each RES unit for all scenarios, which means that the fixed value of this slope can handle all scenarios, even for the worst one. Thus, the optimal control of reactive power from RES inverters is obtained through the two-stage linear stochastic VCC problem.

IV. Numerical Results

We test the proposed LBFS model and two-stage linear stochastic VVC problem in three radial distribution systems. All tests are carried out in MATLAB on a laptop with an Intel Core i5-10500 3.10 GHz CPU and 8 GB of RAM, where the two-stage stochastic optimization is solved using the CPLEX 12.10 optimization studio. The description of test systems is given below.

1) The IEEE 33-bus system: the voltage level is 12.66 kV and the base power is 10 MVA. Other data and network topology for this system are available from Matpower 7.0. The test system is modified with the consideration of non-zero shunt admittance: the shunt conductance is considered the same for the whole system as $Gs = 0.0005$ p.u.; the shunt susceptance Bs is 1/3 of the series impedance magnitude of the same branch [34]. There are three shunt capacitor banks connecting at nodes 6, 24, and 29 with a maximum reactive power capacity as 0.2 p.u.. As for the distributed generators, three RES units with 0.1 p.u. forecasted active power output are installed at nodes 14, 20, and 26. Also, the transformer is located at the substation node of the system.

2) The 95-bus UK generic distribution system (UKGDS95) [35]: the voltage level is 11 kV and the base power is 10 MVA. We modify the shunt admittance the same as the IEEE 33-bus system. There are 3 distributed RES units (at nodes 20, 42, and 95), 3 shunt capacitor banks (at nodes 6, 58, and 73) and 1 transformer (at substation node) in this system. The maximum reactive power capacity of shunt capacitors and forecasted active power output of RES are the same as the IEEE 33-bus system.

3) IEEE 123-bus standard test system (case123): five distributed RES units are installed with the forecasted output of 0.5 MW at nodes 114, 47, 3, 35, and 83. The system originally contains 4 shunt capacitors at nodes 83, 88, 90, and 92. Shunt capacitors can supply a maximum of 250 kvar. Two transformers are integrated in the original system including a substation transformer. Moreover, overhead lines are replaced by underground cables, thus the value of line shunts is increased to 5 times the original one [18]. The three-phase system is transferred into the single-phase system through the positive sequence equivalent and the application of Kron's reduction if the neutral point is also present. The single-phase system in Matpower format is provided by [36].

In the three test systems, the distributed RES units are set in their maximum power point tracking (MPPT) schedule to achieve the highest active power output. The forecasted value of RES active power in each scenario is generated from the probability distribution function between its minimum and maximum values. As for the forecasted value of real-time system load and forecasted error of RES active power, they obey the Gaussian distribution. All the test systems have a transformer located at the substation node, with the tap changer placed on the high voltage winding of transformers. Each tap changer has 13 set points (one at center rated tap and six to increase and decrease the turn ratio). As for shunt capacitor banks, these are made up of a combination of ten capacitor steps connected in parallel. All the test systems are expanded to 100 scenarios with different load power (generated from Gaussian distribution for each scenario) to verify the performance of linear models in large-scale distribution systems at light-, normal-, and heavy-load levels.

A. LBFS Error Analysis

A linearized branch flow model with line shunts (LBFMS) from [23] is linearized through ignoring squared current magnitude l_{jk}. The aforementioned LBFMS model, LFB, and the widely used linear DistFlow model (LinDist) are used to test the performance of LBFS. The results of absolute errors of three linear models are calculated as $error = |linear - ACPF|/ACPF$. V_{AC} and I_{AC} are the voltage and current magnitudes obtained from the ACPF model which already considers non-zero shunt elements. Thus, LinDist, LBF, LBFMS, and LBFS are compared with the benchmark ACPF model to validate the accuracy of obtained solutions. The objective function of PF-based problems using linear models and ACPF is power loss minimization, which is common in solving PF problems. The comparison of calculation accuracy and computing time are shown in Table I. V_e, I_e, and Pl_e are the average errors of voltage magnitude, branch current magnitude, and power loss, respectively, and $\overline{V}_e$ is the largest voltage magnitude error. The results of ACPF are the average actual values in p.u. over all scenarios, and $\overline{V}_e$ is the average actual value of voltage magnitude at the largest error point of LBFS over all scenarios.

According to Table I, it is obvious that all three indices of LBFS are smaller than its counterparts. LBFS exhibits an improvement in the calculation accuracy, which is very important in distribution system analysis and is the main purpose to introduce line shunts into LBF. We can observe a certain decrease in the average error and the largest error point from both LBF and LinDist to LBFS. There are nearly 20%-30% improvements in the accuracy of nodal voltage magnitude in LBFS when compared with those of LBF, especially higher in IEEE 33-bus system which has long distribution feeders, resulting in larger line series impedance and shunt admittance. Moreover, the two reactive power compensators located at nodes 30 and 32 in IEEE 33-bus system increase the error of branch flow, thereby causing the higher error in voltage magnitude. As for the largest voltage error, LBFS achieves a significant improvement compared with other two models.

TABLE I
COMPARISON OF CALCULATION ACCURACY AND COMPUTING TIME (% FOR LINEAR MODELS AND P.U. FOR ACPF)

Test model	IEEE 33-bus system					UKGDS95					IEEE 123-bus standard test system				
	V_e	$\overline{V}_e$	I_e	Pl_e	Time (s)	V_e	$\overline{V}_e$	I_e	Pl_e	Time (s)	V_e	$\overline{V}_e$	I_e	Pl_e	Time (s)
LinDist	4.580	9.180	24.700	26.400	1.27	1.870	5.140	19.300	25.800	4.75	0.740	1.160	10.700	18.600	5.40
LBF	6.010	10.100	27.900	29.600	1.34	1.670	5.000	21.600	24.800	4.88	0.720	1.080	12.100	14.800	5.27
LBFMS	1.680	5.030	13.400	15.800	1.64	1.120	2.030	8.130	8.640	5.21	0.680	1.130	6.470	8.130	6.22
LBFS	1.690	4.170	14.100	15.400	1.53	0.430	1.120	6.780	8.330	4.93	0.510	1.080	8.380	10.100	5.99
ACPF	0.979	0.983	0.115	0.196	24.70	1.019	1.024	0.059	0.150	58.80	0.996	0.994	0.038	0.014	67.20

With regard to the average errors of branch current and power loss, although LBFS still has a relatively higher error, around 10%-15%, it is noted that it does improve a lot from LinDist and LBF, which is nearly 60% enhancement. We believe that this error can be accepted if the load condition is normal or light, and the accuracy of branch current is not the major concern of the fast calculation and estimation of large distribution systems. Perhaps a direct way to improve this shortcoming of accuracy in branch current is modifying the basic LBF model with the consideration of phasor angles instead of just adapting the magnitude parts, which will be discussed in our future work. Moreover, LBFMS shows a higher accuracy than LBFS in branch flow (power loss), but lower accuracy in voltage magnitude. Thus, LBFS shows its own strength of calculation accuracy compared with another linear model with line shunts.

According to Table I, though LBFS considers extra line shunt and transformers, its computing time is nearly the same as that of LBF and smaller than that of LBFMS. Because of the shared linearity, the computing time of LinDist is similar with other linear models. Therefore, LBFS with transformers shows a decent performance not only in the calculation accuracy of nodal voltage magnitude, branch current, and power loss, but also in the high computating efficiency in large radial distribution systems.

B. Effect of Network Reverse PF

The effect of network reverse PF is a non-negligible issue for LBF models. Some warm-start LBF models only consider the single-direction branch flow from former nodes to latter nodes. The reverse PF would potentially cause huge errors of nodal voltage and branch flow (power or current) in these models. In this case, the effect of network reverse PF should be tested to verify the performance of LBFS.

The test is mainly performed in the IEEE 123-bus standard test system, which has several generation power injections at different nodes, and thereby has reverse PFs. For the purpose of the proper comparison, we modify the IEEE 123-bus standard test system by turning off all the RES units. Thus, the reverse PFs are prevented in the modified test system. The simulation results are shown in Fig. 5.

According to Fig. 5, the reverse PF increases the error of nodal voltage magnitude and decreases the calculation accuracy of LBFS. However, the maximum error of nodal voltage magnitude is still lower than 1%, which is accepted as the normal error for qualified linear branch flow models.

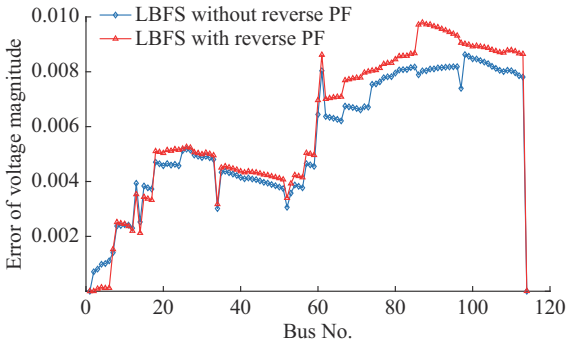

Fig. 5. Error comparison of nodal voltage magnitude of LBFS with and without reverse PF in IEEE 123-bus standard test system.

Therefore, the reverse PF has little influence on the calculation accuracy of LBFS.

C. Two-stage Stochastic Optimization

As previously described in Section I, the "charging effect" caused by the capacitive susceptance of shunt admittance would lift the nodal voltage magnitude, potentially cause voltage violations at certain nodes and affect the safe operation and reliability in power distribution systems. This claim is tested in the IEEE 33-bus system with and without line shunts. As shown in Fig. 6, the nodal voltage magnitude increases because of the "charging effect" from non-zero shunt elements. Furthermore, the voltage magnitude may easily break the upper limit and cause violations if the system exists nodal power injection from the distributed generators, like RES units. Therefore, we propose a two-stage scenario-based optimization problem to control the voltage magnitude within the operating limits considering RES output uncertainties.

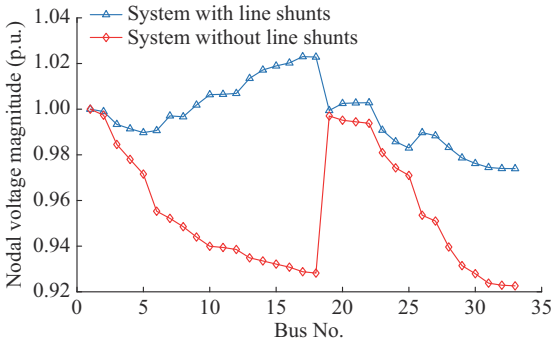

Fig. 6. Nodal voltage magnitude of IEEE 33-bus system.

The two-stage scenario-based VVC problem based on LBFS is a linear program, thus the problem with a large number of scenarios, $N_s = 10000$, can be solved directly within a single optimization framework. By setting such a big number of scenarios, we ensure that all possible real-time RES output uncertainties are handled though the two-stage optimization problem. Table II gives the value of the element in the linear decision rule. The slope of the decision rule of all scenarios m varies between negative and positive values to adjust the forecasted error for the optimal schedule of reactive power from RES.

TABLE II
VALUE OF ELEMENT IN LINEAR DECISION RULE

System	Case	$Q^0_{RES,1}$ (p.u.)	m_1	$Q^0_{RES,2}$ (p.u.)	m_2	$Q^0_{RES,3}$ (p.u.)	m_3
IEEE 33-bus system	Deterministic	0.252	0	0.174	0	0.182	0
	Adjustable		0.079		0.098		0.092
UKGDS95	Deterministic	0.128	0	0.185	0	0.309	0
	Adjustable		0.098		0.086		–0.107
IEEE 123-bus standard test system	Deterministic	0.246	0	0.041	0	0.127	0
	Adjustable		–0.103		0.085		0.132

Table III provides the values of discrete control variables in the VVC problem, where k^{real} is the real value of transformer voltage ratio based on the simulation result k. We assume each capacitor bank has a step length of 0.02 p.u., and each transformer tap ratio has a step length of 0.001 p.u.. Q^{real}_{Cap} and k^{real} are the real discrete control values used for the VVC problem. Figure 7 shows the nodal voltage magnitude of the IEEE 33-bus system before and after implementing VVC problem (randomly taking one scenario as an example). Obviously, the primary purpose of implementing VVC problem, which is limiting voltage magnitude within stable operating region, is achieved. Also, VVC based on LBFS can avoid the violation in voltage magnitude caused by interactions of RES units and the "charging effect" caused by non-negligible capacitive susceptance. In conclusion, VVC based on LBFS achieves the expected outcome in voltage control.

TABLE III
VALUES OF DISCRETE CONTROL VARIABLES

System	Q_{Cap} (p.u.)	Q^{real}_{Cap} (p.u.)	k	k^{real}
IEEE 33-bus system	0.1918	0.20	1.0009	1.001
	0.0389	0.04		
	0.0188	0.02		
UKGDS95	0.1782	0.20	1.0014	1.001
	0.0597	0.06		
	0.0925	0.10		
IEEE 123-bus standard test system	0.2000	0.20	1.0019	1.002
	0.0467	0.04		
	0.0724	0.08		

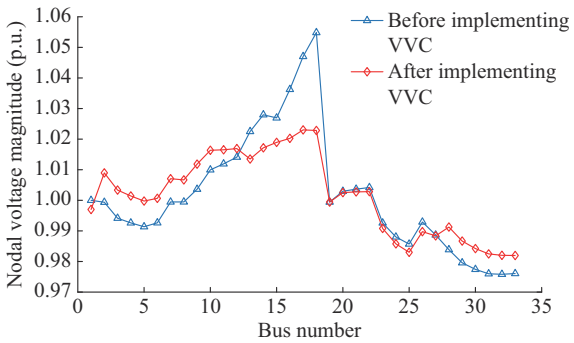

Fig. 7. Nodal voltage magnitude of IEEE 33-bus system before and after implementing VVC.

Table IV illustrates the computing time of the three test systems. Taking the IEEE 123-bus standard test system as an example, the solving time of the two-stage scenario-based VVC problem (adjustable case) is around 32 min. The traditional VVC problem with such large number of scenarios would cost several hours to be solved. For example, the solving time of chance-constraint VVC problem with only 18 scenarios based on ACPF with SOCP tested in the IEEE 123-bus standard test system is 210.63 s [24]. Therefore, this highlights the importance of the LBFS based two-stage scenario-based VVC problem in saving computing time.

TABLE IV
COMPUTING TIME OF THREE TEST SYSTEMS

System	Computing time (s)	
	Deterministic case	Adjustable case
IEEE 33-bus system	91.843	1044.32
UKGDS95	186.752	1754.98
IEEE 123-bus standard test system	222.445	1934.61

Three indices are introduced to further demonstrate the effectiveness of the proposed two-stage linear stochastic VVC problem and are defined as follows.

1) Scenario failure rate (SFR) is the ratio of scenarios with voltage violations among all scenarios:

$$SFR = \frac{N_{sVV}}{N_s} \tag{34}$$

2) The maximum voltage violation value $VV_{\max}$ is the difference between the maximum/minimum voltage violation point and the upper/lower limit.

3) Voltage violation probability (VVP) is the probability of all nodal voltage violations of all scenarios:

$$VVP = \frac{\sum_{s=1}^{N_s} n_{VVs}}{N_B N_s}$$

4) Conservative index (CI) is defined as the increase in the expected power loss for the stochastic two-stage VVC schedule from that of the base schedule:

$$CI = \frac{loss_{adj} - loss_{det}}{loss_{det}}$$

The values of the security constraint indices are given in

Table V. According to the first three indices, it is noted that the base case would have a large number of voltage and branch flow (current) violations N_{sIV} because of the unexpected forecasted errors of RES, while the increasing numbers of voltage and current violations have been almost eliminated by the two-stage VVC problem through the linear decision rule. Taking the IEEE 123-bus standard test system as an example, around 11% of scenarios have at least one nodal voltage violation under the base case schedule, and the SFR is decreased to 1.4% after the two-stage case schedule. Also, the same situation goes for VVP, whose value decreases from 4.41% to around 0.39%, and the maximum voltage violation value decreases from 0.024 p.u. to 0.0011 p.u.. Therefore, the robustness of controlling voltage magnitude through the two-stage scenario-based VVC problem is established. Moreover, the expected power loss of two-stage VVC problem is increased slightly compared with that of the deterministic case. This small increasing cost of conservativeness can be accepted because the robustness is our key concern in distribution systems.

TABLE V
VALUES OF SECURITY CONSTRAINT INDICES

System	Case	N_{sVV}	N_{sIV}	*SFR* (%)	$VV_{\max}$ (p.u.)	*VVP* (%)	Power loss (p.u.)	*CI* (%)
IEEE 33-bus system	Deterministic	783	134	7.83	0.0130	3.47	1.32	4.54
	Adjustable	81	33	0.81	0.0012	0.14	1.38	
UKGDS 95	Deterministic	1015	182	10.15	0.0180	4.12	1.59	5.35
	Adjustable	69	35	0.69	0.0014	0.28	1.68	
IEEE 123-bus standard test system	Deterministic	1123	201	11.23	0.0240	4.41	1.66	6.02
	Adjustable	140	79	1.40	0.0011	0.39	1.76	

V. CONCLUSION

This paper proposes an LBFS in radial distribution systems. LBFS, as the first linear π equivalent circuit model considering shunt elements of lines and transformers, exhibits linearity and high computating efficiency compared with traditional ACPF and other models with line shunts like LBFMS, and achieves enhanced accuracy compared with linear DistFlow and LBF models. Extensive simulation tests are conducted to prove the improvement of LBFS in calculating nodal voltage magnitude (the precise requirement in distribution systems). Besides, the network reverse PF is tested to have nearly no influence on LBFS. Moreover, a linear two-stage linear stochastic VVC problem based on LBFS considering the uncertainty in active power output of RES is formulated in this paper. The primary purposes of implementing VVC method are limiting the voltage magnitude within stable operating region and avoiding the violation in voltage magnitude caused by interactions of distributed generators (RES units) and the "charging effect" caused by non-negligible capacitive susceptance, which are achieved through this modelling framework. The proposed two-stage linear VVC problem can adjust the reactive power output according to active power fluctuations through the linear decision rule of fast control devices viz. RES inverters, in addition to deciding the set points of the classical voltage control devices. Numerical studies prove that the proposed two-stage linear stochastic VVC problem exhibits a better performance in eliminating voltage violations than the traditional deterministic case, while it has some acceptable increase in conservativeness (system power loss). The two-stage linear stochastic VVC problem based on LBFS preserves linearity and convexity, thus the computing efficiency is significantly improved when compared with traditional ACPF-based stochastic VVC methods.

REFERENCES

[1] Z. Yang, H. Zhong, A. Bose *et al.*, "A linearized OPF model with reactive power and voltage magnitude: a pathway to improve the MW-only DC OPF," *IEEE Transactions on Power Systems*, vol. 33, no. 2, pp. 1734-1745, Mar. 2018.

[2] T. Yang, Y. Guo, L. Deng *et al.*, "A linear branch flow model for radial distribution networks and its application to reactive power optimization and network reconfiguration," *IEEE Transactions on Smart Grid*, vol. 12, no. 3, pp. 2027-2036, May 2021.

[3] K. Purchala, L. Meeus, D. Van Dommelen *et al.*, "Usefulness of DC power flow for active power flow analysis," in *Proceedings of IEEE PES General Meeting*, San Francisco, USA, Jun. 2005, pp. 454-459.

[4] M. E. Baran and F. F. Wu, "Network reconfiguration in distribution systems for loss reduction and load balancing," *IEEE Power Engineering Review*, vol. 9, no. 4, pp. 101-102, Apr. 1989.

[5] A. Garces, "A linear three-phase load flow for power distribution system," *IEEE Transactions on Power Systems*, vol. 31, no. 1, pp. 827-828, Jan. 2015.

[6] H. Yuan, F. Li, Y. Wei *et al.*, "Novel linearized power flow and linearized OPF models for active distribution networks with application in distribution LMP," *IEEE Transactions on Smart Grid*, vol. 9, no. 1, pp. 438-448, Jul. 2016.

[7] X. Chen, W. Wu, and B. Zhang, "Robust capacity assessment of distributed generation in unbalanced distribution networks incorporating anm techniques," *IEEE Transactions on Sustainable Energy*, vol. 9, no. 2, pp. 651-663, Sept. 2018.

[8] J. Zhang, M. Cui, B. Li *et al.*, "Fast solving method based on linearized equations of branch power flow for coordinated charging of EVS (EVCC)," *IEEE Transactions on Vehicular Technology*, vol. 68, no. 5, pp. 4404-4418, Mar. 2019.

[9] D. Liu, L. Liu, H. Cheng *et al.*, "An extended DC power flow model considering voltage magnitude," *Journal of Modern Power Systems and Clean Energy*, vol. 9, no. 3, pp. 679-683, Jan. 2021.

[10] T. Yang, Y. Guo, L. Deng *et al.*, "A distribution system loss allocation approach based on a modified DistFlow model," in *Proceedings of 2020 IEEE PES General Meeting*, Montreal, Canada, Aug. 2020, pp. 1-5.

[11] Z. Yang, K. Xie, J. Yu *et al.*, "A general formulation of linear power flow models: basic theory and error analysis," *IEEE Transactions on Power Systems*, vol. 34, no. 2, pp. 1315-1324, Sept. 2019.

[12] H. Lin, X. Shen, Q. Guo *et al.*, "Accuracy and application scope analysis for linearized branch flow model in radial distribution systems," in *Proceedings of 2021 IEEE PES General Meeting*, Washington DC, USA, Jul. 2021, pp. 1-5.

[13] S. Haffner, L. F. A. Pereira, L. A. Pereira *et al.*, "Multistage model for distribution expansion planning with distributed generation – part I: problem formulation," *IEEE Transactions on Power Delivery*, vol. 23, no. 2, pp. 915-923, Mar. 2008.

[14] J. Teng, "A direct approach for distribution system load flow solutions," *IEEE Transactions on Power Delivery*, vol. 18, no. 3, pp. 882-887, Jul. 2003.

[15] S. H. Low, "Convex relaxation of optimal power flow? Part I: formulations and equivalence," *IEEE Transactions on Control of Network Systems*, vol. 1, no. 1, pp. 15-27, Mar. 2014.

[16] S. Bose, S. H. Low, T. Teeraratkul *et al.*, "Equivalent relaxations of optimal power flow," *IEEE Transactions on Automatic Control*, vol. 60, no. 3, pp. 729-742, Sept. 2015.

[17] E. M. Baran and F. F. Wu, "Optimal capacitor placement on radial distribution systems," *IEEE Transactions on Power Delivery*, vol. 4, no.

1, pp. 725-734, Jan. 1989.
[18] G. Zha, Y. Yuan, Z. Fu *et al.*, "Reactive compensation of offshore wind farm considering charging power of the submarine cable," *Power System and Clean Energy*, vol. 29, pp. 1-7, May 2013.
[19] T. A. Papadopoulos, D. A. Tsiamitros, and G. K. Papagiannis, "Impedances and admittances of underground cables for the homogeneous earth case," *IEEE Transactions on Power Delivery*, vol. 25, no. 2, pp. 961-969, Mar. 2010.
[20] T. Noda, "Numerical techniques for accurate evaluation of overhead line and underground cable constants," *IEEJ Transactions on Electrical and Electronic Engineering*, vol. 3, no. 5, pp. 549-559, Sept. 2008.
[21] K. Christakou, D. C. Tomozei, J. Boudec *et al.*, "AC OPF in radial distribution networks – parts I, II," *Computer Science*, vol. 143, no. 6, pp. 276-288, Mar. 2015.
[22] M. Nick, R. Cherkaoui, J. Y. Leboudec *et al.*, "An exact convex formulation of optimal power flow in radial distribution networks including transverse components," *IEEE Transactions on Automatic Control*, vol. 63, no. 3, pp. 682-697, Mar. 2017.
[23] F. Zhou and S. H. Low, "A note on branch flow models with line shunts," *IEEE Transactions on Power Systems*, vol. 36, no. 1, pp. 537-540, Oct. 2021.
[24] F. U. Nazir, B. C. Pal, and R. A. Jabr, "A two-stage chance constrained volt/var control scheme for active distribution networks with nodal power uncertainties," *IEEE Transactions on Power Systems*, vol. 34, no. 1, pp. 314-325, Jul. 2018.
[25] R. A. Jabr, "Power flow based volt/var optimization under uncertainty," *Journal of Modern Power Systems and Clean Energy*, vol. 9, no. 5, pp. 1000-1006, Sept. 2021.
[26] R. Jabr, "Optimal placement of capacitors in a radial network using conic and mixed integer linear programming," *Electric Power Systems Research*, vol. 78, no. 6, pp. 941-948, Jun. 2008.
[27] M. B. Liu, C. A. Canizares, and W. Huang, "Reactive power and voltage control in distribution systems with limited switching operations," *IEEE Transactions on Power Systems*, vol. 24, no. 2, pp. 889-899, Mar. 2009.
[28] A. Borghetti, "Using mixed integer programming for the volt/var optimization in distribution feeders," *Electric Power Systems Research*, vol. 98, pp. 39-50, May 2013.
[29] R. Liang and C. Cheng, "Dispatch of main transformer ULTC and capacitors in a distribution system," *IEEE Transactions on Power Delivery*, vol. 16, no. 4, pp. 625-630, Oct. 2001.
[30] A. Augugliaro, L. Dusonchet, S. Favuzza *et al.*, "Voltage regulation and power losses minimization in automated distribution networks by an evolutionary multiobjective approach," *IEEE Transactions on Power Systems*, vol. 19, no. 3, pp. 1516-1527, Aug. 2004.
[31] R. Jabr and I. Džafić, "Penalty-based volt/var optimization in complex coordinates," *IEEE Transactions on Power Systems*, vol. 37, no. 3, pp. 2432-2440, Oct. 2022.
[32] H. Ahmadi, J. R. Mart, and H. W. Dommel, "A framework for volt-var optimization in distribution systems," *IEEE Transactions on Smart Grid*, vol. 6, no. 3, pp. 1473-1483, Dec. 2014.
[33] R. Jabr, "Linear decision rules for control of reactive power by distributed photovoltaic generators," *IEEE Transactions on Power Systems*, vol. 33, no. 2, pp. 2165-2174, Aug. 2018.
[34] W. H. Kersting, "Shunt admittance of overhead and underground lines," in *Distribution System Modeling and Analysis*, Boca Raton: CRC Press, 2017.
[35] Y. P. Agalgaonkar, B. C. Pal, and R. A. Jabr, "Distribution voltage control considering the impact of PV generation on tap changers and autonomous regulators," *IEEE Transactions on Power Systems*, vol. 29, no. 1, pp. 182-192, Sept. 2014.
[36] M. Nick, R. Cherkaoui, J.-Y. L. Boudec *et al.*, "An exact convex formulation of the optimal power flow in radial distribution networks including transverse components," *IEEE Transactions on Automatic Control*, vol. 63, no. 3, pp. 682-697, Jun. 2018.

Hanyang Lin received the B.S. degree in electrical engineering from Hefei University of Technology, Hefei, China, in 2020, and the M.Sc. degree in electrical and electronic engineering from Imperial College London, London, U.K., in 2021. He is currently pursuing the Ph.D. degree in electrical and electronic engineering in Tsinghua-Berkeley Shenzhen Institute, Tsinghua Shenzhen International Graduate School, Tsinghua University, Shenzhen, China. His research interests include electricity market, virtual power plants, and modeling and stability analysis of distribution systems.

Firdous Ul Nazir received the B.Tech. degree in electrical engineering from the National Institute of Technology, Srinagar, India, in 2012, the M.Tech. degree in electrical power systems from Indian Institutes of Technology, Roorkee, India, in 2015, and the Ph.D. degree from Imperial College London, London, U.K., in 2020. He is currently working as a Lecturer of electrical power engineering with the Department of Electrical and Electronic Engineering, Glasgow Caledonian University, Glasgow, U.K.. His current research interests include distribution system modeling, operation and control, and optimization theory.

Bikash C. Pal received the B.E.E. (with honors) degree from Jadavpur University, Calcutta, India, the M.E. degree from the Indian Institute of Science, Bangalore, India, and the Ph.D. degree from Imperial College London, London, U.K., in 1990, 1992, and 1999, respectively, all in electrical engineering. He is currently a Professor with the Department of Electrical and Electronic Engineering, Imperial College London. He is a Fellow of the IEEE for his contribution to power system stability and control. His current research interests include renewable energy modelling and control, state estimation, and power system dynamics.

Ye Guo received the bachelor's and Ph.D. degrees from the Department of Electrical Engineering, Tsinghua University, Beijing, China, in 2008 and 2013, respectively. He is an Associate Professor with Tsinghua-Berkeley Shenzhen Institute, Tsinghua Shenzhen International Graduate School, Tsinghua University, Shenzhen, China. He was a Postdoctoral Associate with Cornell University, Ithaca, USA, from 2014 to 2018. From 2019 to 2021, he won the IEEE PES General Meeting Best Paper Awards four times for three years in a row and one co-authored paper selected as the "Best-of-the-Best Paper Award." He has also won the Best Paper Awards for IEEE EI^2 Conference in 2020 and 2021 and the Best Poster Award for PSERC IAB Meeting 2018. His research interests include optimal dispatch, market mechanisms, and machine learning for power and energy systems.